Countries most exposed to individual and compound extremes at different global warming levels

Fulden Batibeniz[1], Mathias Hauser[1], Sonia I. Seneviratne[1]

[1]Institute for Atmospheric and Climate Science, Department of Environmental Systems Science, ETH Zurich, Zurich, Switzerland

Correspondence to: Fulden Batibeniz (fulden.batibeniz@env.ethz.ch)

Abstract. It is now certain that human-induced climate change is increasing the incidence of extreme temperature, precipitation and drought events globally. A critical aspect of these extremes is their concurrency that may result in substantial impact on society and environmental systems. Therefore, quantifying compound extremes in current and projected climate is necessary to take measures and adapt to future challenges. Here we investigate pre-industrial and projected changes of individual and concurrent extremes using multi-model simulations of the 6th phase of the Coupled Model Intercomparison Project (CMIP6). We focus on individual and simultaneous occurrence of extreme events: heat wave, drought, maximum 1-day precipitation (Rx1day) and extreme wind (wind) in the pre-industrial period (1850-1900) and at four global warming levels (GWLs of +1°C, +1.5°C, +2°C and +3°C). We find that, on a global scale, most investigated individual extremes become more frequent and affect more land area for higher GWLs. This increase differs depending on the considered months and implies both unprecedented shifts in timing and disproportional increases in frequency of concurrent events for different climate regions. As a result, concurrent occurrences of the investigated extremes become 2.7 to 8.1 times more frequent for a GWL of 3°C. At +3°C the most dramatic increase is identified for concurrent heat wave-drought events with an eight-fold increase in subtropical countries, a seven-fold increase in northern middle and high latitude countries, and a five-fold increase in tropical countries, respectively. Our results also suggest that years without any individual events will decrease six-fold while the number of years with two concurrent events will double. Given the projected disproportional frequency increases across GWLs and decreasing non-event years, our results strongly emphasize the risks of uncurbed greenhouse gas emissions.

Plain Language Summary

We study single and concurrent extreme heatwaves, droughts, maximum precipitation, and strong wind events. Globally, these extremes become more frequent and affect larger land areas under future warming. Only a few years would go by without any extremes. Heat waves-droughts are projected to increase the most in subtropical countries, whereas this is the case for high precipitation-wind in the tropics. More people will be exposed to these extreme events unless mitigation actions are urgently taken.

30

1. Introduction

The socio-economic impacts of individual and concurrent extremes are accelerating as the climate changes (IPCC, 2021). The intervals between extremes are becoming shorter which puts vulnerable communities and ecosystems at risk. In addition, while most countries are affected by climate extremes, some economies such as in south and southeast Asia are
35 more vulnerable than advanced economies in the northern hemisphere (Guo et al., 2021). These emerging challenges motivate the need for a comprehensive analysis of potential changes in exposure to individual and concurrent extremes on the population- and country-level.

Human-induced climate change is now exacerbating climate extremes in every region across the globe (Seneviratne et al., 2021). This increase in climate extremes cannot be explained without human influence and threatens both developed
40 countries and developing countries. For instance, Puerto Rico, Myanmar, Haiti, Philippines, Mozambique, the Bahamas, Bangladesh, Pakistan, Thailand and Nepal are the ten most affected countries from climate extremes in terms of economic and environmental fatalities in the last two decades (Eckstein et al., 2021). This indicates the inequity between CO_2 emitter and non-emitter countries to deal with climate-induced risks and impacts. Additionally, it is estimated that over 475'000 people lost their lives and 2.56 trillion[5] USD (in purchasing power parity) of losses were incurred as a direct result of more
45 than 11'000 extreme events between 2000 and 2019 (Eckstein et al., 2021). This indicates an urgent need to assess climate-induced risks and impacts regionally.

The damage that extreme events cause is not only related to the frequency, severity or magnitude of the events but also to socioeconomic factors (Botzen et al., 2010; Frame et al., 2020; Jahn, 2015, IPCC, 2021) such as land use, income, education, employment and community safety. Different economic and social structures will alter the adaptive capacity to climate
50 change. This makes it difficult to disassociate climate-related hazards from socioeconomic factors. Even so, assuming that projected future changes will take place in a world with a society and economy similar to today would help to understand the relative impacts of climate change on exposure.

Previous studies primarily focus on current and/or projected changes of extremes such as extreme temperatures, precipitation, or drought (Batibeniz et al., 2020a; Forzieri et al., 2016; Kelebek et al., 2021). Recently, compound events -
55 multiple extremes occurring either simultaneously or/and consecutively - have become an important topic due to the rising awareness about their possible amplified impacts (Mazdiyasni and AghaKouchak, 2015; Seneviratne et al., 2010; Zscheischler and Seneviratne, 2017). Many recent studies have also discussed the possible increase in compound event frequency in the future climate (Saeed et al., 2021; Schwingshackl et al., 2021; Vogel et al., 2017, 2020). The impacts associated with compound events are expected to be higher than impacts caused by individual extremes. For example, a
60 combination of extreme wind and extreme precipitation can increase the destruction of infrastructure and economic losses. As climate change alters the nature of individual extremes, compound events composed of individual extremes are expected

to be unprecedented in terms of severity and intensity (Seneviratne et al., 2021). This emerging understanding makes quantifying the projected changes in the characteristics of compound events necessary.

A range of obstacles hinders reliable likelihood estimation of compound events. Extreme events are rare by definition and
65 compound events even more so. Additionally, a robust understanding and detailed spatiotemporal information on exposure to multivariate extremes requires detailed spatiotemporal information. This hinders the assessment of observation-based compound events. Therefore, large model ensembles (Champagne et al., 2020; Poschlod et al., 2020; Ridder et al., 2021; Vogel et al., 2020), process-based model simulations (Couasnon et al., 2020) and reanalysis data (Martius et al., 2016) can complement observational data when spatio temporal coverage is not sufficient. In particular, multi-GCM ensembles capture
70 the uncertainty in the large-scale climate and can be a useful tool to investigate compound events in current and future climate.

In this study, we investigate the individual occurrences of heat waves, droughts, extreme precipitation and extreme wind as well as compound heat wave-drought, and extreme precipitation and extreme wind events, all of which can have severe impacts on different sectors. The first combination - heat wave-drought - influences wildfire, crops, natural vegetation,
75 power plants and fisheries (Zscheischler et al., 2020). The second combination - extreme wind and precipitation - can cause storm surges, floodings, runoff, and result in the destruction of infrastructure and damage to the economy. Heat wave-drought occurrences have increased in the last four to five decades (Alizadeh et al., 2020; Feng et al., 2020; Hao et al., 2018; Kong et al., 2020; Li et al., 2020; Manning et al., 2019; Mazdiyasni and AghaKouchak, 2015; Mukherjee and Mishra, 2021; Ridder et al., 2020; Sarhadi et al., 2018; Schubert et al., 2014; Sharma and Mujumdar, 2017; Wu et al., 2021; Zhou and Liu,
80 2018; Zscheischler and Seneviratne, 2017; Kirono et al., 2017) and are projected to increase in the future (Diffenbaugh et al., 2015; Herrera-Estrada and Sheffield, 2017; Li et al., 2019; Sedlmeier et al., 2018). This increase is mostly attributed to the increase in heat wave occurrences (Bevacqua et al., 2022). Indeed, even when droughts alone do not display an increasing tendency, compound occurrences of heat waves and drought events are expected to increase (Sarhadi et al., 2018; Yu and Zhai, 2020). Compound precipitation and wind extremes have also been investigated in the observational period over many
85 regions including the Mediterranean Basin (Raveh-Rubin and Wernli, 2015), Europe (De Luca et al., 2020; Zscheischler et al., 2021), Great Britain (Tilloy et al., 2021), and at the global scale (Martius et al., 2016; Messmer and Simmonds, 2021). However, these studies differ in methodology, time and spatial scale and future changes of precipitation-wind extremes have, to the best of our knowledge, not been covered in the compound event context.

Building on previous work on projected changes in compound extreme events, we investigate here for the first time the
90 human exposure to these concurrent extremes in addition to individual extremes. We do so in a manner consistent with the 6th Assessment Report of the Intergovernmental Panel on Climate Change (IPCC AR6) framework by analyzing the projections for different global warming levels (GWLs, +1°C, +1.5°C, +2°C and +3°C) on country and regional scales. We analyze simulations from 17 climate models from the CMIP6 archive to investigate the occurrence of individual and compound events under natural climate variability and future global warming. To estimate exposure, we use current
95 population estimates provided by the Gridded Population of the World version 4 (GPWv4) data set (Center for International

Earth Science Information Network - CIESIN - Columbia University, 2018). Together, the use of climate change projections and population distributions enables the investigation of changes in the exposure to climate extremes at the regional and country levels.

2. Data and Methods

2.1 Climate model data

We use CMIP6 simulations (Eyring et al., 2016) of 17 climate models to perform individual and concurrent event analysis in pre-industrial period (1850-1900) and at four GWLs (see below) for the shared socioeconomic pathway (SSP) projection marking the high end of future forcing pathways (SSP5-8.5) (Jones and O'Neill, 2020; Jones and O'Neill, 2016). The SSP5-8.5 experiment also represents high mitigation and low adaptation challenges resulting in radiative forcing of 8.5 W/m^2 by the end of 2100. Because we present our results at GWLs we do not expect our results to strongly depend on the choice of the scenario (Seneviratne et al., 2016; Seneviratne and Hauser, 2020; Wartenburger et al., 2017). We use the same ensemble member (r1i1p1f1) of each model. We retrieve daily maximum temperature, precipitation, wind and monthly soil moisture data from each model and use second order conservative remapping (Jones, 1999) to regrid them onto a common 2.5° x 2.5° longitude-latitude grid to enable comparison across different models. The full list of models is provided in Table A1.

2.2. Population Counts

We use gridded population counts retrieved from Gridded Population of the World version 4 (GPWv4). GPWv4 provides population distributions on various grid resolutions and we make use of the 1° resolution data in our population exposure analysis. To match the resolution of the climate data, we also transform gridded population data into 2.5° grid resolution using second order conservative remapping. GPWv4 data is available for the period from 2000 to 2020 at 5 year intervals. In this paper 2015 population counts are used to represent the world population for +1°C of global warming. We also use population projections from the Shared Socio-Economic Pathway 5 (SSP5; Jones and O'Neill, 2020; Jones and O'Neill, 2016), which are available from 2000 to 2100 in 10-year intervals. We linearly interpolate both SSP5 and GPWv4 in time to obtain annual population counts and to compare the two datasets.

2.3 Climate Regions

We focus our analysis on three climatic macro regions: Northern Middle and High Latitude Countries (MHC), Subtropical Countries (STC), Tropical Countries (TRC) (Fig. 1). Climate regions are aggregated country polygons. To compile these regions, we consider latitudinal location, in addition to climate patterns affecting the countries. The assessments are performed and presented both in regional and country scale to emphasize the response of different climatic regions/countries to individual and compound extremes. We use climate regions in section 3.1-3.2 figures and country polygons in section 3.3-3.5 figures.
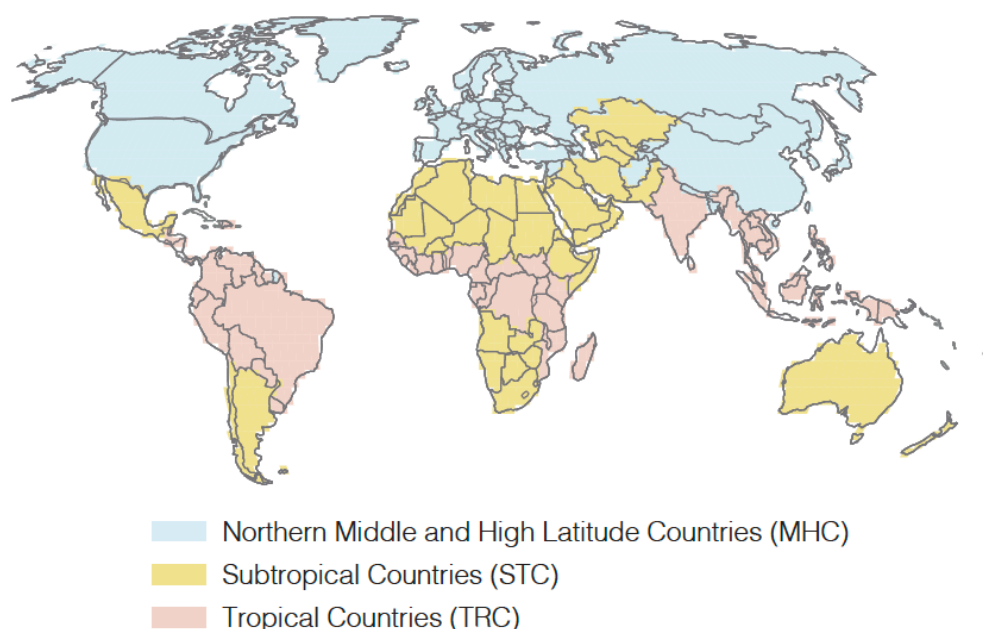
Figure 1. World map is divided into 3 climatic macro regions: Northern Middle and High Latitudes Countries (MHC), Subtropical Countries (STC), and Tropical Countries (TRC).

2.4 Global temperature and warming level calculation

We perform our analysis considering +1°C, +1.5°C, +2°C and +3°C global warming levels to be consistent with the IPCC AR6 context (Seneviratne et al., 2021). The warming levels are defined as the first 30-year period where global mean temperature anomalies exceed the given temperature (e.g. +2.0°C). We consider 1850 to 1900 as our reference period and compute anomalies relative to this time period. We refer the reader to Seneviratne and Hauser, (2020) for detailed information regarding the calculation of global warming levels.

2.5 Definition of individual events

For our analysis we analyse heat waves, droughts, heavy precipitation, and high wind events. In a first step we compute climate indices and then count the extreme events based on their 10th/ 90th percentiles during the reference period (1850-1900).

All the calculations are performed on the grid basis. Since drought events are on the monthly timescale (see below) we aggregate the other extreme events to a monthly timescale as well. If one or more daily events happen in a month it is marked as an "event month", otherwise it is a "non-event month".

Heat wave: We use daily maximum temperature to determine heat wave events. We first calculate the 90th percentile for each calendar day using a 31-day moving window over the reference period 1850-1900. We then identify the day as a heat wave event if the daily max temperature exceeds the daily 90th percentile for at least five consecutive days.

150 Drought: We compute drought using monthly soil moisture data. We use soil moisture to define drought events because it directly represents water availability, in contrast to many other measures (e.g. the standardized precipitation index, SPI) that are based on precipitation scarcity (Seneviratne et al., 2010). We first normalize soil moisture by subtracting the mean of each month and dividing it by its standard deviation over the reference period. We then compute the 10th percentile for each calendar month over the reference period. The month is then defined as a drought event if it falls below its 10th percentile.

155 Rx1day: We use daily precipitation to calculate monthly maximum 1-day precipitation events. We find the maximum 1-day precipitation of each month in the reference period and define the 90th percentile for each calendar month. Heavy precipitation events are then defined as the days where precipitation is above the monthly threshold.

Extreme wind: We use average daily wind speed to calculate extreme wind. For the 90th percentile calculation we use monthly maximum wind speeds in the reference period. Extreme wind speed days are then defined as days where daily wind
160 speed is above the 90th percentile.

2.6 Definition of compound events

We define compound events as events that occur in the same month and affect the same location. In this context, we define two types of concurrent events: combined heat wave and drought events as well as Rx1day and extreme wind events. Thus,
165 if a specific month experiences two individual events, it is marked as "event month", for that grid cell and month. Note that the individual extremes that comprise concurrent events are first calculated separately. We then mark the time step and grid points where both hazards simultaneously occur in the same month.

3. Results

170 ### 3.1 Future changes in individual and concurrent extremes over the climate regions

We illustrate the development of the investigated events with the help of Venn diagrams, which allows us to analyse the individual and concurrent exceedances at the same time. We visualize the individual events by circles and their concurrency by the intersection of the circles. The displayed results represent the regional and multi-model mean. We thereby focus on three continental climate regions (MHL, STC, TRC) for pre-industrial, current (+1°C) and future climate (+1.5°C, +2°C, and
175 +3°C) (Fig. 2a,b).

At the current warming level the heat wave frequency almost doubled compared to pre-industrial levels in MHC and STC, and it tripled in TRC (Table 1). The event fraction at +3.0°C is higher in MHC (40.9%, 3.1 times more compared to pre-industrial levels), however, the proportional increase is higher in TRC (40.6%, 3.9 times more compared to pre-industrial levels). Drought events, on the other hand, tend to decrease for higher GWLs in MHC and STC. Even though the number of
180 individual droughts decreases, the total number of droughts (individual+concurrent) increases across all climate regions
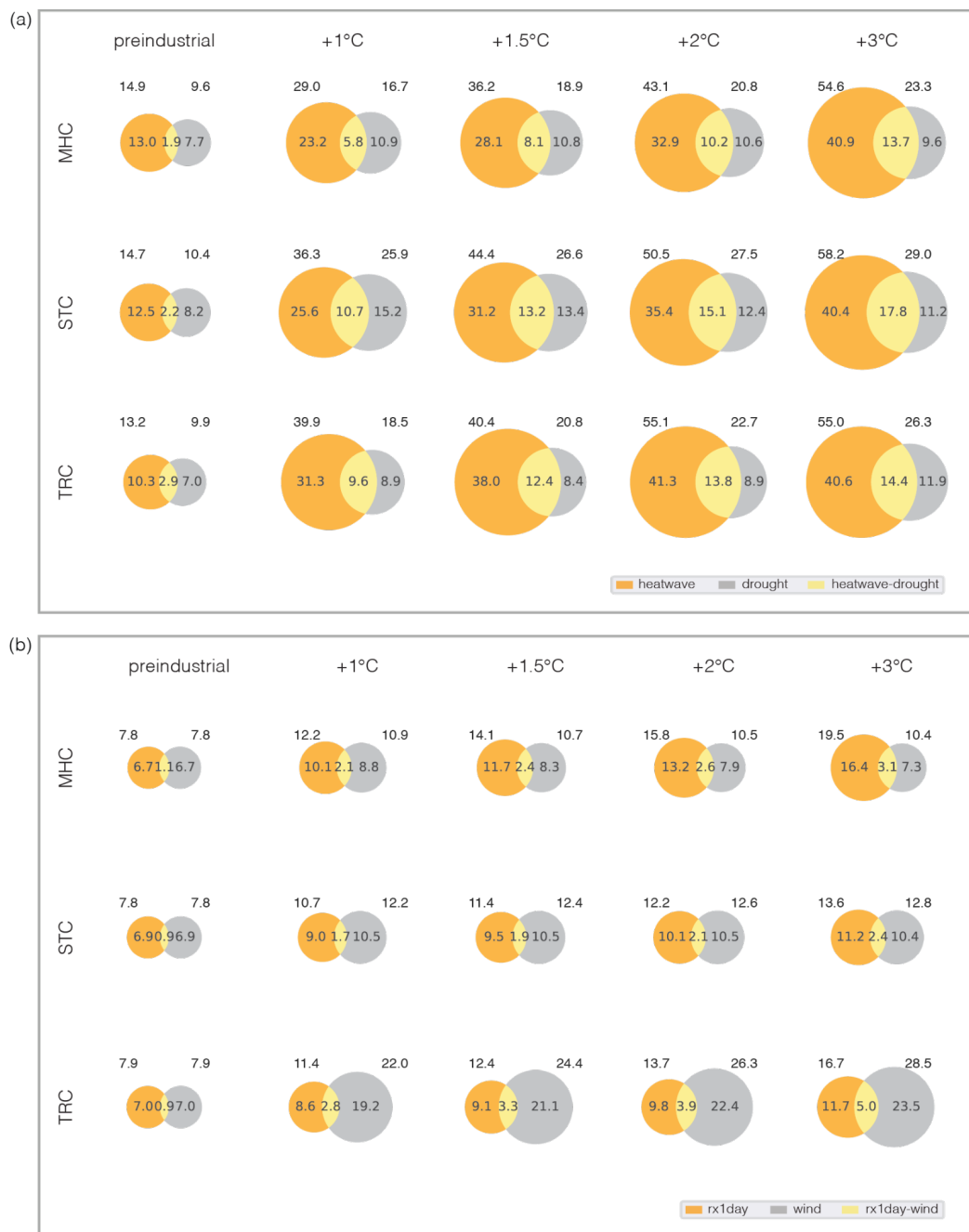
Figure 2. Venn diagrams of (a) heatwave-drought and (b) Rx1day-wind storm events at global warming levels. The values show the individual and concurrent frequency of events in MHC, STC and TRC in preindustrial period and at +1°C, +1.5°C, +2°C and +3°C GWLs. Areas of the circles are proportional to the frequencies [%] and represent the multi-model mean. The numbers above the Venn diagrams represent the total share of individual events including the ones occurring during concurrent events.

Table 1. Increase in individual and concurrent events at global warming levels relative to pre-industrial levels.

	MHC			STC			TRC		
	hw	hw-drought	drought	hw	hw-drought	drought	hw	hw-drought	drought
+1°C	1.8	3.1	1.4	2.0	4.9	1.9	3.0	3.3	1.3
+1.5°C	2.2	4.3	1.4	2.5	6.0	1.6	3.7	4.3	1.2
+2°C	2.5	5.4	1.4	2.8	6.9	1.5	4.0	4.8	1.3
+3°C	3.1	7.2	1.2	3.2	8.1	1.4	3.9	5.0	1.7
	MHC			STC			TRC		
	Rx1day	Rx1day-wind	wind	Rx1day	Rx1day-wind	wind	Rx1day	Rx1day-wind	wind
+1°C	1.5	1.9	1.3	1.3	1.9	1.5	1.2	3.1	2.7
+1.5°C	1.7	2.2	1.2	1.4	2.1	1.5	1.3	3.7	3.0
+2°C	2.0	2.4	1.2	1.5	2.3	1.5	1.4	4.3	3.2
+3°C	2.4	2.8	1.1	1.6	2.7	1.5	1.7	5.6	3.4

190   which corresponds to an increase by a factor ~2.5 (at +3°C) compared to the pre-industrial period. Concurrent heat wave and drought events are projected to increase in all climate regions with higher GWLs. At the current global warming level, the number of events are projected to occur about 3 times more frequently for MHL and TRP and 4.9 times more frequently for STC compared to the pre-industrial period. The strongest increase across the warming levels occurs for STC. It gradually increases by a factor of 4.9, 6.0, 6.9, and 8.1 for +1°C, +1.5°C, +2°C, and +3°C relative to pre-industrial levels. This sharp

195   increase is followed by MHL, where the fraction of events is 1.9% at pre-industrial levels, 5.8% at current GWL and 13.7% at +3°C of global warming, corresponding to 3.1 (7.2) times more heat wave-drought events than pre-industrial periods at +1°C (+3°C). In TRP, the frequency of concurrent heat wave-drought events increases by a factor of 3.3, 4.3, 4.8 and 5.0 for +1°C, +1.5°C, +2°C, and +3°C with respect to pre-industrial levels.

   In Fig. 2b, we show Rx1day and wind events. The most dramatic increase in individual Rx1day events is detected in MHC.

200   The frequency of Rx1day events gradually increases across the warming levels by a factor of 1.5, 1.7, 2.0 and 2.4 for +1°C, +1.5°C, +2°C, and +3°C with respect to pre-industrial levels. The hotspot for individual wind events is TRC. The increase

reaches 2.7 times at +1°C GWL and continues to increase to 3.0, 3.2 and 3.4 for +1.5°C, +2°C, and +3°C. For MHL and STC, individual wind events show an increasing tendency up to +1.5°C and start to decrease at +2°C and +3°C. However, the total number of events (individual+concurrent) increased for STC, while it decreased for MHC. On the other hand,

205 concurrent Rx1day and wind events are already twice the pre-industrial levels at 1°C warming and it is projected to increase further for 3°C GWL. Even though the percentage of concurrent events is less compared to individual events, the relative increase is larger across warming levels. Concurrent Rx1day-wind event fractions are projected to increase 5.6 times for TRP, 2.8 times for MHC and 2.7 times for STC at +3°C GWL.

210 **3.2 Timing of individual and concurrent extremes**

To gain further insights on future individual and concurrent extremes over the climate regions, we now focus on their frequency and timing for each calendar month under pre-industrial conditions and at GWLs (Fig. 3 and 4).

Again, we first consider heat wave and drought events (Fig. 3). As expected, heat waves increase strongly with global warming (Fig. 3, top row). At +1°C of global warming, the associated changes are already far beyond the conditions from

215 pre-industrial levels and show further gradual increase across the global warming levels. Heat waves increase inhomogeneously across months. This unequal distribution leads to much larger increases in some months than the annual average suggests (Fig. 2). The increase is especially inhomogenous for MHC. At +1°C of global warming, heat wave events occur mostly in spring and summer. However, for higher GWLs there is a sharp increase for most months except May and June. In STC and TRC, the increase across warming levels is more homogenous, with a slight shift towards summer months

220 in STC.

Due to its structure, drought indicates more continuous increase across months for all regions (Fig. 3, middle row). The most dramatic increase of drought is observed for summer months in MHC, while STC and TRC show a relatively homogenous increase over the months. Interestingly, STC sees a small decrease in individual drought events in most months for 3°C warming.

225 The development of concurrent heat wave-drought events is not simply the combination of the individual events (Fig. 3, bottom row). They also show a general increase which, however, has some distinct features. The pattern in MHC is especially interesting: the months July, August, and September indicate a sharp increase, while October, November, and December show practically no increase. Other months are between the extremes. For STC, the frequency increase is maximum in September followed by February at +3°C. In the case of TRC, our results indicate that the distribution across

230 months changes from 2°C to 3°C. The months July to August show a decrease in frequency for +3°C compared to +2°C, whereas for November and December it is an increase in frequency.
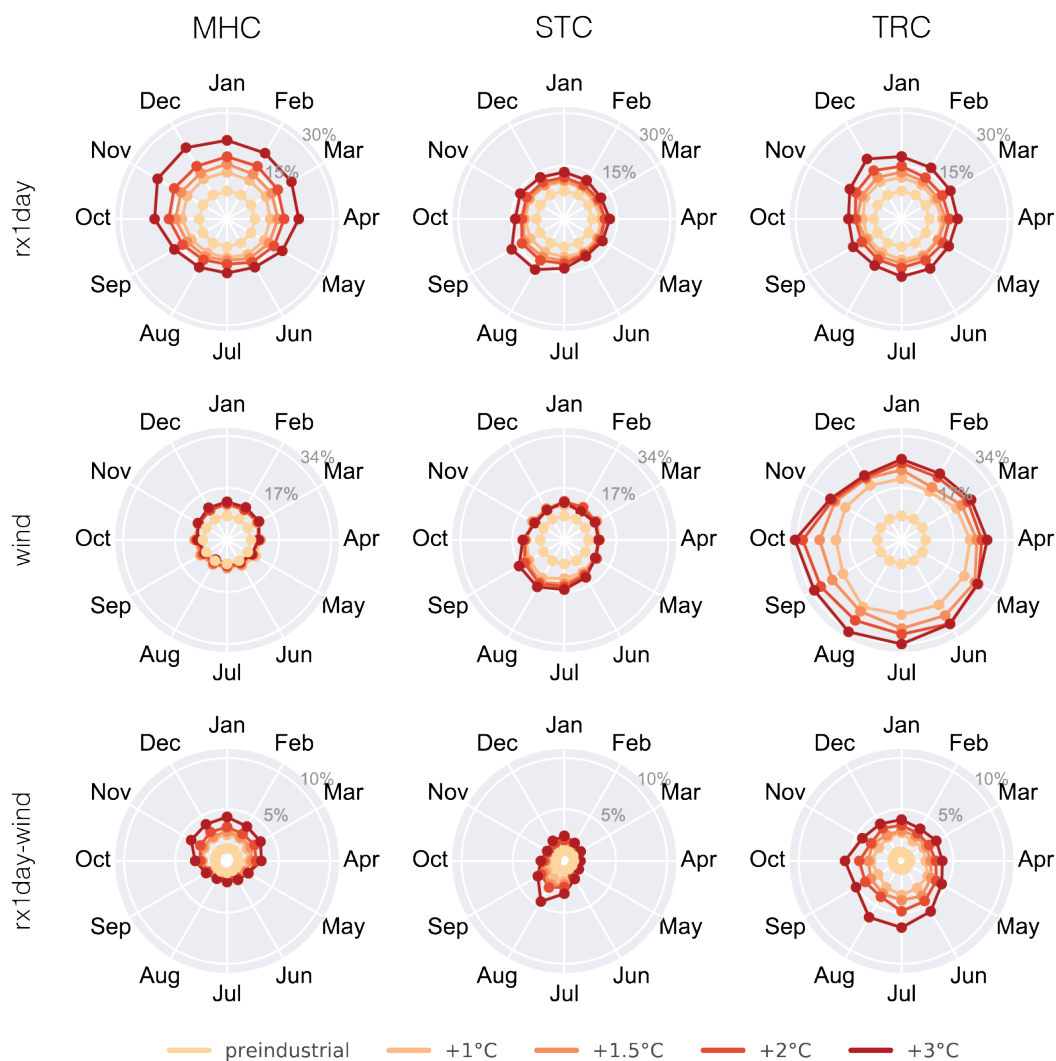
The increase in Rx1day, wind and Rx1day-wind events is observed across all months and warming levels (Fig. 4). The increase is more even than for the heat wave and drought events. However, in some regions it is not linear across months. Individual occurrences of Rx1day events are on the rise across the GWLs and regions. At +3°C of global warming, MHC

235 indicates the highest increase in months between September and May. The increase is more homogenous for STC and TRC.

Nonetheless, events seem to increase the most in September and August for STC and December for TRC for the highest GWL. Wind extremes vary more compared to Rx1day events across the regions. The most dramatic increase is identified in TRC from June to October. The second most increase in frequency is observed for STC followed by MHC. In STC, July, August and September seem to be the months where the highest frequency increase is observed. These increases in

240 individual event frequencies leads to a difference among the regions for concurrent Rx1day-wind events. While there is an increase in winter and spring for MHC, there is an increase in July for STC and all months but especially June to September in TRC.
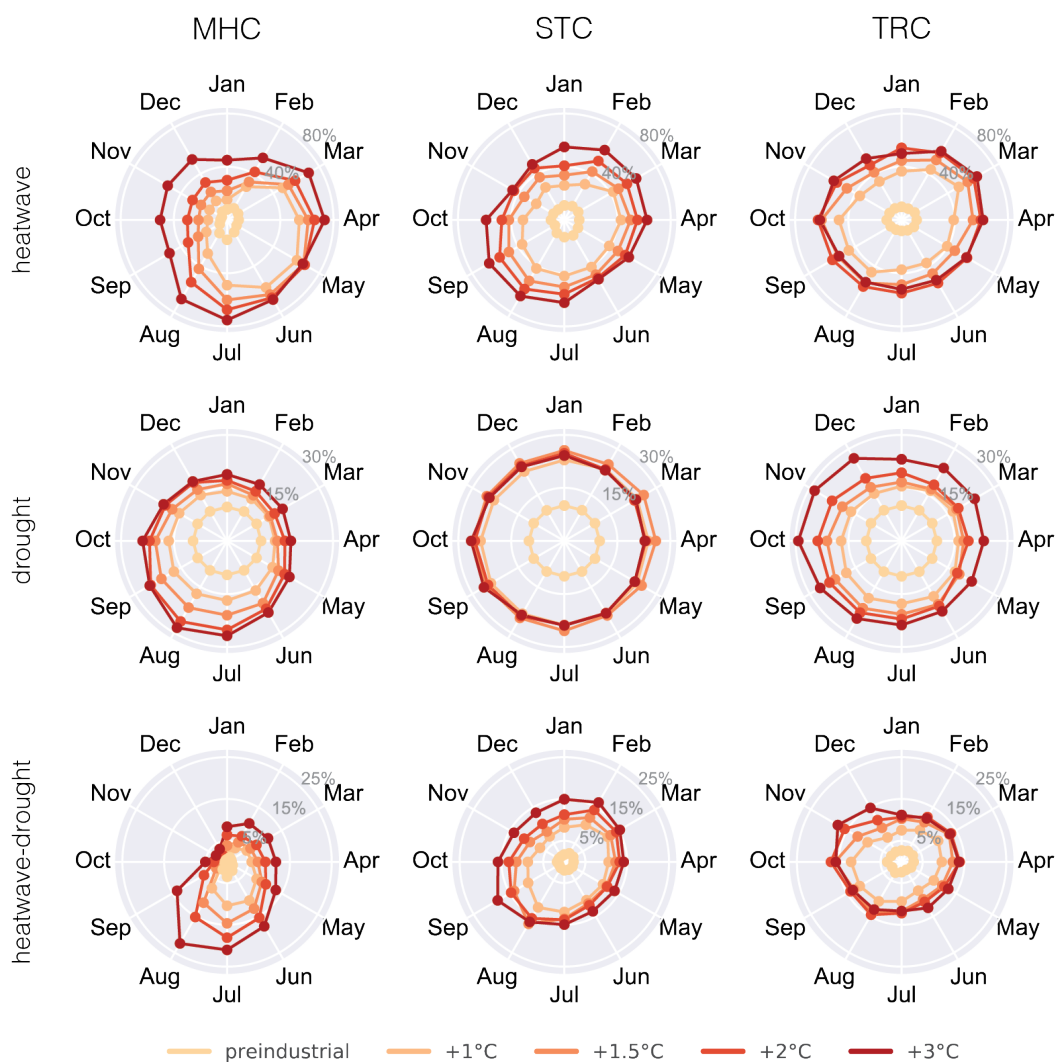
245 **Figure 3.** Timing and frequency of heat wave, drought, and concurrent heat wave-drought events in MHC, STC and TRC at preindustrial period and at +1°C, +1.5°C, +2°C and +3°C global warming levels.

**Figure 4.** Same as Fig. 3 but for Rx1day, wind and concurrent Rx1day-wind events.

3.3 Hotspot of Changes in Individual and Concurrent Extremes

This section presents the potential hotspots that are prone to an increase in exposure to multiple hazards in a future climate (Fig. 5). We performed this analysis for the four individual event types (Fig. 5 [a]) and the two concurrent event types (Fig. 5 [b]) at GWLs. The first row shows how many of the event types increased at least 20% relative to the reference period, and the second row shows how many of the event types increased at least 100% (i.e. a doubling of the event frequency).

Considering the individual extremes with the lower threshold (20%; Fig. 5[a], top row), three out of four individual extremes are projected to increase across almost the entire globe - even at a GWL of 1°C. Many regions, including South America, Canada, China, some subtropical countries in North and South Africa and some Mediterranean countries, display change in

260 all four individual extremes at 3°C GWL (Fig. B1. [a]). For the higher threshold and +1°C of global warming, two out of four individual events already doubled pre-industrial levels over South America and the tropical countries of Africa. This increase is projected to continue and affect more land area for higher GWLs. The most prominent hotspots of change are Brazil, the United States and China where the common drivers are heat waves and drought (Fig. B1. [a]).
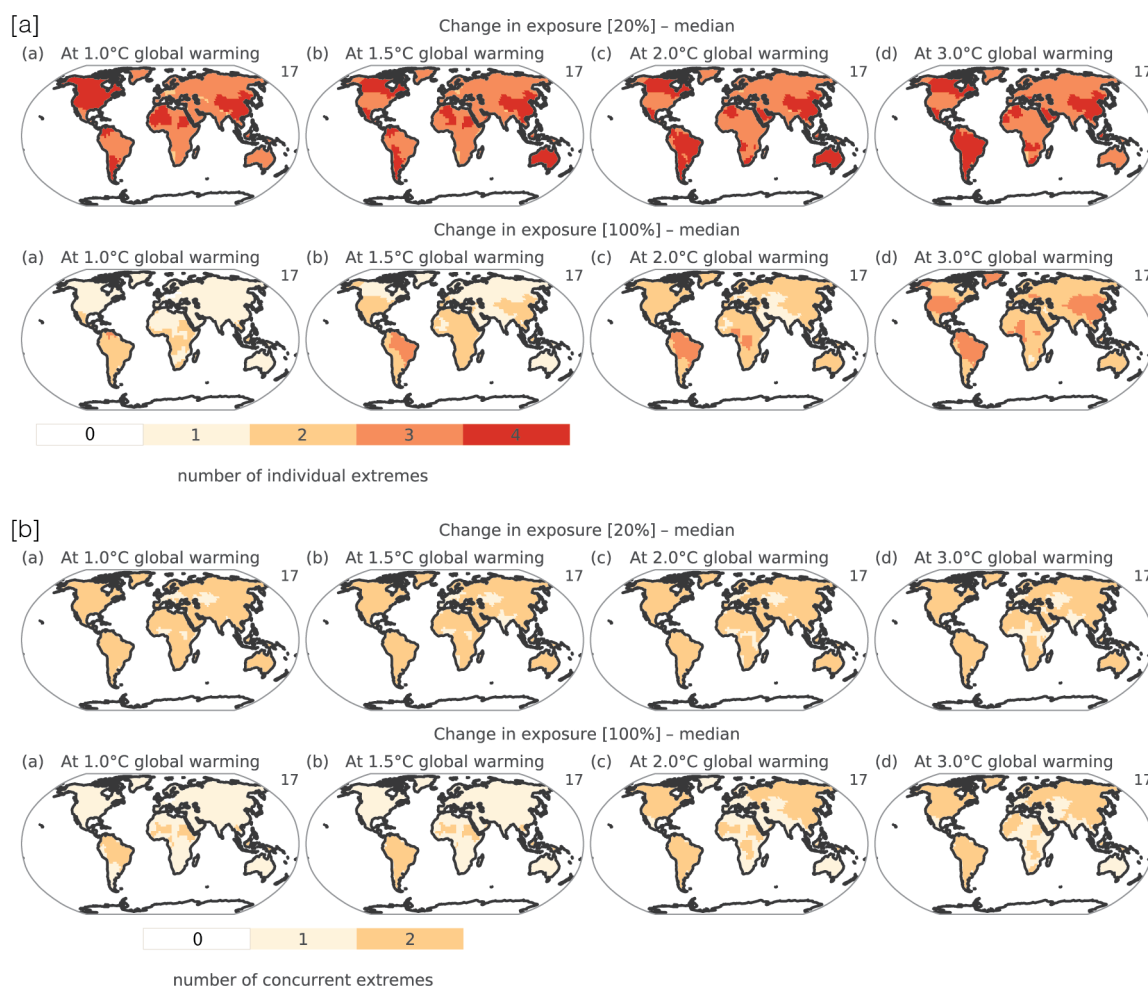
Figure 5. Area exposed to 1, 2, 3 or 4 individual extremes (heatwave, drought, Rx1day, wind) with relative increases over 20% (top row) and 100% (bottom row) with respect to the pre-industrial period [a] and area exposed to 1 or 2 concurrent extremes (heatwave-drought, Rx1day-wind) with relative increases over 20% (top row) and 100% (bottom row) with respect to the pre-industrial period [b].

270

Two concurrent extreme pairs display a 20% increase at all GWLs across the globe except some countries in Africa, Central Asia, as well as India (Fig. 5 [b] top row). The northern part of South America and some tropical countries in Africa already

double the pre-industrial levels of heat wave-drought and Rx1day-wind frequency at 1°C warming (Fig. 5 [b] bottom row).
The regions where only one event doubles in frequency are mostly driven by heat wave-drought events (Fig. B1. [b]).

275 Starting from 2°C of global warming both extreme pairs permanently double the pre-industrial levels for a large proportion
of the globe. Rx1day-wind events occurring in Mexico, western and central Europe, some countries surrounding the
Mediterranean Sea and Australia do not contribute to 100% change, whereas for some tropical countries in Africa,
Kazakhstan and India its heat wave-drought events do not contribute to 100% change.

3.4 Population Exposure

280

Projected changes in individual and concurrent occurrences of heat wave, drought, Rx1day and wind events suggest a
growing risk for population exposure across the globe. In addition, the global population is expected to continue its growth,
further exacerbating the risk for human and natural systems. For example, SSP5 projects the average world population to
grow from 7.29 billion in 2015 to its maximum in 2060 (8.6 billion) and decrease thereafter to about 7.4 billion people by

285 2100 - the lowest population size among SSPs (Fig. B2) (Jones and O'Neill, 2020; Jones and O'Neill, 2016). However, to
estimate the population exposure on a country-by-country basis we use 2015 levels (7.33 billion) provided in the Gridded
Population of the World version 4 (GPWv4) data. Thus, in this study, we don't consider increasing population from SSP5
but hold it constant at 2015 levels for a number of reasons. (i) Comparing GPWv4 with SSP5 projections suggest that the
population in 2015 is 39 million people higher (7.29 billion) in SSP5 than in GWPv4 with an even higher discrepancy for

290 2020 (Fig. B2). (ii) Population projections are given for time periods while we report our results for global warming levels.
Because each GCM reaches a warming level for a different time period it would be difficult to assign a population number to
the GWL. (iii) The projected population in SSP5 is strictly larger than in 2015, which suggests that our exposure based on
2015 population is conservative and gives a lower estimate.

Fig. 6 shows the number of events per person on the country basis. The first column represents the current (+1°C) number of

295 events per person and the second, third and fourth columns show the projected changes in the number of events at +1.5°C,
+2°C and +3°C GWLs with respect to +1°C. Even when not taking the expected rise in the human population into account,
increases in extremes alone are projected to increase the event number per person in most countries. For +1°C of global
warming, heat wave events range between 100 and >250 events per person. The number of events per person increases by
~20-50 events for +1.5°C, ~50-100 events for +2°C and ~50->100 events for +3°C GWL. The most vulnerable countries for

300 heat wave events are Australia and South Africa. The most vulnerable countries for drought are the Mediterranean countries,
India, China, Australia, the United States and northwestern parts of South America. Furthermore, the number of drought
events per person seems to be the least recurring event around the tropical countries in Africa and India. Concurrent heat
wave-drought events range between 20 and 200 events per person across the globe for +1°C of global warming. The number
of events per person increases gradually across the globe except tropical countries in the African continent and India. The

305 most dramatic increase is observed for countries in the Mediterranean Basin. The number of events tend to increase for all
the countries in MHC, South America and Australia up to more than 100 events per person.
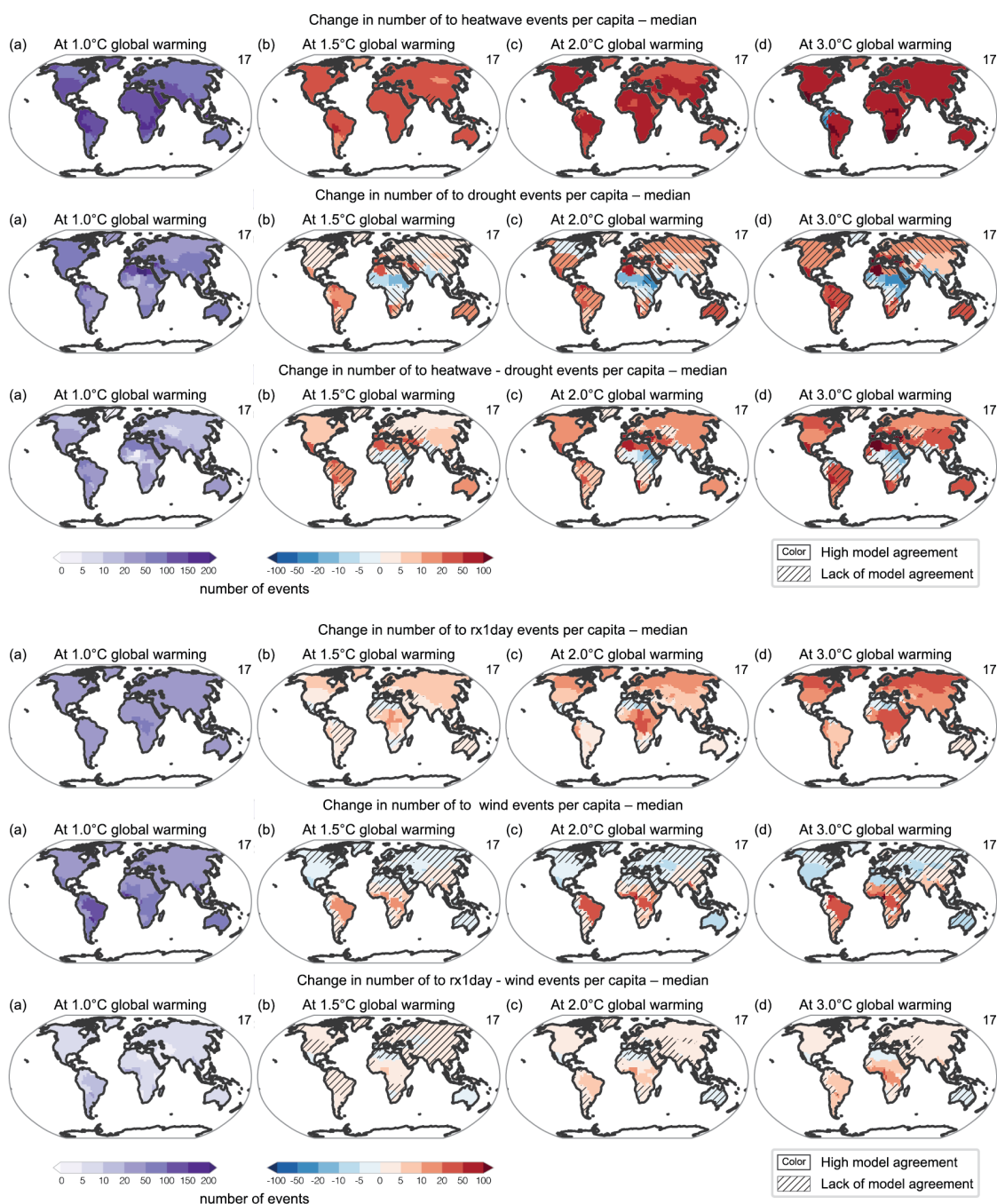
Figure 6. Number of individual and concurrent extremes per capita (a) at +1°C and (b, c, d) change at +1.5°C, +2°C and +3°C with respect to +1°C. 2015 population counts have been used for the analysis. Colors refer to high model agreement and hatched areas refer to lack of model agreement.

Individual Rx1day and wind events numbers per person are not variable across the globe for +1°C of global warming

315 (mostly 50-100 or more). The number of Rx1day events per person is on the rise for higher global warming levels except Mediterranean countries and southern parts of the African continent, which even show a small decrease. At +2°C of global warming, Rx1day events increase the most for tropical countries in the African continent. This increase continues for +3°C global warming almost everywhere across the globe. Wind extremes are also increasing mostly for tropical countries including South America, tropical countries on the African continent, and India. Most of the MHC and STC countries

320 experience a decrease in the number of events per person down to 20 events for higher global warming levels. The number of events per capita for concurrent Rx1day and wind events are increasing across the globe, except the countries in the Mediterranean Basin and Australia. We observe the highest increase over the tropical countries in Africa up to 50-100 events.

325 **3.5 Non-event Years**

Fig. 7 shows the number of "normal" (i.e. non-event) years that countries experience – i.e. the number of years without any individual and concurrent events studied in this paper (median of GCMs). We calculate the number of non-event years over the 30 year period comprising the GWLs. In the case of individual events, there are between 3 and 17 normal years. For +1°C of global warming, the number of normal years has already decreased to around 6 years for some countries. The

330 countries with the least normal years are the northern part of South America and tropical and subtropical countries in the African continent and the Mediterranean countries. For higher GWLs, some countries evolve to become a hotspot with less normal years. This decrease is dramatic for the northern part of South America, especially Brazil. Another vulnerable region is the Mediterranean Basin where the number of normal years decreases from 11 to 2 (i.e. maximum for Spain). Overall, the number of normal years decreases by around 5 years from +1°C to +1.5°C, 7 years from +1.5°C to +2°C, and 10 years from

335 +2°C to +3°C.

Years without concurrent events range between 29 and 15 across warming levels. The number of non-event years decreases by around 4 years from +1°C to +1.5°C, 7 years from +1.5°C to +2°C, and 10 years from +2°C to +3°C. Hotspots for these changes are projected in the countries surrounding the Mediterranean Sea where the maximum change occurs for Jordan (from 26 to 16 normal years), followed by Spain, Greece, Tunisia, Macedonia, Turkey, Syria, Portugal and Italy. Northern

340 parts of South America especially Bolivia, Chile, Paraguay and Brazil, South Africa, the United States of America, Australia and Mexico are also very vulnerable to this change.

15
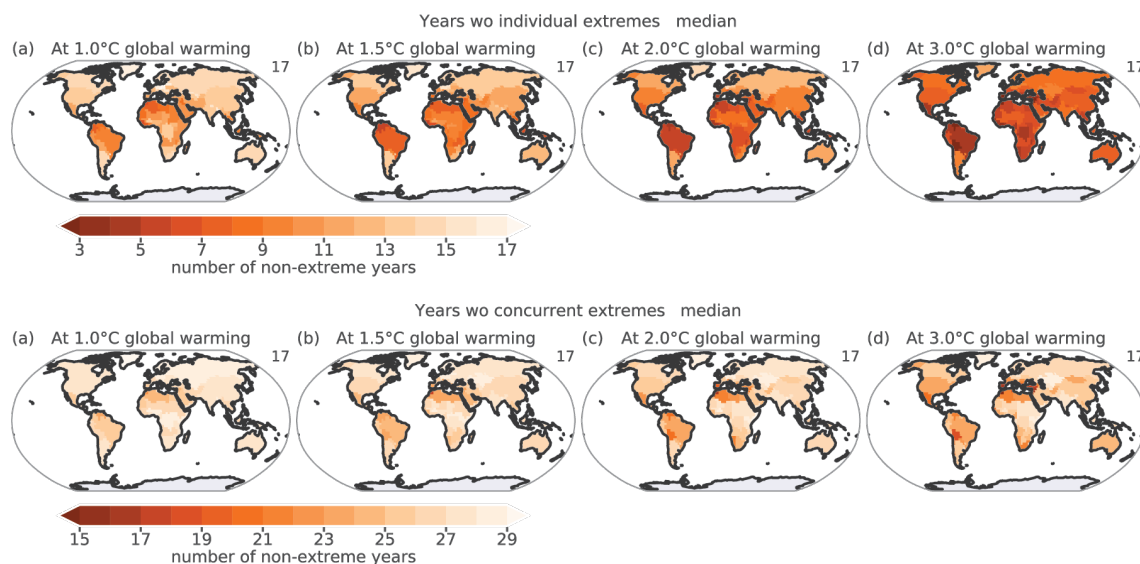
Figure 7. Normal years: Number of years without individual (top row) and concurrent (bottom row) extremes in MHC, STC and TRC at warming levels (+1°C, +1.5°C, +2°C and +3°C).

4. Discussion

Our results highlight the increasing frequency of heat waves, droughts, Rx1day and wind extremes with global mean warming. These findings, in particular the respective spatial patterns and increasing signals, are in accordance with the findings of the IPCC AR6 report. In the IPCC AR6 report, projected changes in annual maximum daily precipitation (Rx1day) and annual maximum temperature (TXx) indicate an increase over almost all land areas while soil moisture drought shows a heterogeneous pattern (Seneviratne et al. 2021). Additionally, mean wind is expected to increase gradually in the 21st century in some tropical regions and decrease for the rest of the global land areas (Ranasinghe et al. 2021). In this work, individual heat waves, Rx1day and wind extremes present consistent results with the above mentioned indices. In addition to the drying regions in the IPCC AR6 we found two more drought-prone regions: China and the Arabian Peninsula. Increasing occurrence of these individual extremes can have important implications for natural and human systems. Therefore, the compatibility between the IPCC report and our results increase the confidence in our estimates of concurrent extremes that are associated with even more severe effects than the respective individual extremes.

With higher global warming levels, we have seen a sharp increase in concurrent heat wave-drought events in three climate regions with the most dramatic increase in STC followed by MHC (Fig. 3a). As opposed to heat wave-drought events, Rx1day-wind events increase the most in TRC (Fig. 3b). The frequency differences among regions can be explained by varying climatic regimes. For instance, STC is more affected by warm-dry conditions than TRC because arid climate zones have more climate variability than equatorial climate zones. Another reason behind the frequency differences across regions can be the underlying dynamical and thermodynamic processes such as atmospheric circulation and teleconnection patterns.

16

365 For example, compound droughts are associated mainly with El Niño Southern Oscillation (ENSO) (Singh et al., 2021) and wet and windy extremes in north-western Europe are associated with the positive phase of the North Atlantic Oscillation (NAO) (De Luca et al., 2020). Another key mechanism responsible for frequency increase can be the interaction between land and atmosphere (Seneviratne et al., 2010). Lack of moisture during droughts limits land evaporation, which leads to an increase in sensible heat and in turn increases temperatures (Chiang et al., 2018). Furthermore, the changes in moisture

370 sources and sinks due to future increases in greenhouse gas forcing will likely alter the hydrologic cycle (Batibeniz et al., 2020b) and such changes will likely intensify the land-atmosphere feedback mechanism causing concurrent warm and dry conditions. Additionally, the enhancement of the concurrent very hot-dry warm seasons in many regions have also been linked with increasing dependence between temperature and precipitation associated with global warming (Zscheischler and Seneviratne, 2017). Moreover, it has been found that future occurrences of compound hot–dry events over land are

375 connected with the variations in precipitation trends (Bevacqua et al., 2022).

Our results highlight the positive trend both in individual and concurrent events with higher global warming levels. The probability of occurrence of compound extremes is much lower than individual extremes by definition. Our results showcase this as individual events overall increase more than compound events. However, the multivariate structure of heat wave-drought and Rx1day-wind events change in the future across all climate regions. The interchangeable relationship between

380 individual and compound events can be a sign of distributional changes in mean climate. In any case, increasing frequency decreases the number of non-event years without any individual/concurrent extreme (Fig. 8) which leaves less and less time for adaptation and recovery. Additionally, timing analysis indicates either abrupt increases or shifts in individual and concurrent extremes (Fig. 4, 5). The inhomogeneous increases and changes in timing pose a risk for different sectors such as agriculture, tourism, health. These changes may serve as a red flag for countries which have a sector-dependent economy.

385 Our analysis indicates that exposure to multivariate extremes are on the rise across the globe. For some countries, there is a dipolar pattern between exposures to heat wave-drought events and Rx1day-wind events. While the Mediterranean countries, Southern Africa and Australia have an increase (decrease) in heat wave-drought (Rx1day-wind) events, Central Africa and India, Southeast Asia have a decrease (increase). Northern and middle high latitude countries and Brazil including the Amazon region are also at great risk. Amazonia, Southern Africa, Sahel, India, and Southeast Asia have been projected as a

390 hotspot for increasing temperatures and are the most vulnerable regions to extreme events (Bathiany et al., 2018). Low-income countries have been found to be more economically vulnerable to weather and climate extremes than rich countries (Dell et al., 2014, 2012; Jones and Olken, 2010). Therefore, these highly populated vulnerable countries that are prone to the largest changes in multi-hazard exposures could potentially be at larger risk. The population living in the urban extent of Europe in 2015 is projected to increase more than 5% by 2050 (United Nations et al., 2019) and SSP population projections

395 also estimate an increase in population (Jones and O'Neill, 2016). Therefore, using population projections to investigate the human contribution to the change could help understand future risks more (Batibeniz et al., 2020a; Mukherjee et al., 2021). Our results provide evidence for an already existing vulnerability that may further increase in regions where extreme events will become more frequent due to climate change.

400 **5. Conclusions**

Investigating future changes in impactful individual and concurrent extremes is important to be prepared for future climate risks. In this study, we have investigated the current state and future change of individual and concurrent occurrences of heat wave, drought, Rx1day, wind events at global warming levels (GWLs) of +1°C, +1.5°C, +2°C and +3°C relative to the pre-industrial period for three climate regions. Utilizing simulations from 17 CMIP6 global circulation models allowed us to gain

405 a robust understanding of extremes in current and future climate.

Our results indicate that all climate regions are under the increasing influence of concurrent heat wave-drought events and Rx1day-wind events with higher GWLs. Even though this change is more substantial for heat wave-drought events, Rx1day-wind events are also on the rise. While the most prominent increase is observed in Subtropical Countries (STC) for heat wave-drought events, it is also observed in Tropical Countries (TRC) for Rx1day-wind events. While heat wave-drought

410 events increased substantially, Rx1day-wind events increased less in Northern Middle and High Latitude Countries (MHC) and STC. However in TRC both heat wave-drought and Rx1day-wind events increased at the same rate, indicating the less variable climate in TRC. Our results also highlight the important timing shifts in the occurrence of individual and concurrent extremes in the future climate. Individual extreme events increase inhomogeneously across months leading to unprecedented frequency increases in some months in the future. Another important highlight of our study is increasing human exposure to

415 multivariate extremes in parallel with the decreasing number of non-event years, even without considering the expected rise in the human population.

Quantifying frequency and timing of the individual and concurrent extremes at warming levels provides a perspective to The Paris Agreement's goals that pursue efforts to limit the temperature increase to +2°C (UNFCCC, 2015). Our results suggest that there is a prevailing increase in frequency, shifts in timing of multivariate extremes from +1.5°C to +2°C, that will likely

420 exacerbate human exposure to these extremes. These unprecedented changes in frequency and timing can lead to an elevated risk for the environment and society across the globe. Therefore, our results suggest an urgent need for concrete actions to mitigate current greenhouse gas emissions.

425

430

Appendix A

435 **Table A1.** The list of CMIP6 GCMs

No	GCM Name	Resolution	Ensemble No
1	ACCESS-CM2	native atmosphere N96 grid (144x192 lat x lon)	r1i1p1
2	ACCESS-ESM1-5	native atmosphere N96 grid (145x192 lat x lon)	r1i1p1
3	CMCC-CM2-SR5	native atmosphere regular grid 1deg; 288 x 192 longitude/latitude	r1i1p1
4	CanESM5	T63L49 native atmosphere, T63 Linear Gaussian Grid; 128 x 64 longitude/latitude; 49 levels; top level 1 hPa	r1i1p1
5	EC-Earth3	TL255, linearly reduced Gaussian grid equivalent to 512 x 256 longitude/latitude; 91 levels; top level 0.01 hPa	r1i1p1
6	FGOALS-g3	native atmosphere area-weighted lat x lon grid (80x180 lat x lon)	r1i1p1
7	GFDL-CM4	atmos data regridded from Cubed-sphere (c96) to 180,288; interpolation method: conserve_order2	r1i1p1
8	GFDL-ESM4	atmos data regridded from Cubed-sphere (c96) to 180,288; interpolation method: conserve_order2	r1i1p1
9	INM-CM4-8	gs2x1.5 2x1.5; 180 x 120 longitude/latitude; 21 levels; top level sigma = 0.01	r1i1p1
10	INM-CM5-0	gs2x1.5 2x1.5; 180 x 120 longitude/latitude; 73 levels; top level sigma = 0.0002	r1i1p1
11	IPSL-CM6A-LR	LMDZ grid NPv6, N96; 144 x 143 longitude/latitude; 79 levels; top level 40000 m	r1i1p1
12	MIROC6	native atmosphere T85 Gaussian grid T85; 256 x 128 longitude/latitude; 81 levels; top level 0.004 hPa	r1i1p1
13	MPI-ESM1-2-HR	spectral T127; 384 x 192 longitude/latitude; 95 levels; top level 0.01 hPa	r1i1p1
14	MPI-ESM1-2-LR	spectral T63; 192 x 96 longitude/latitude; 47 levels; top level 0.01 hPa	r1i1p1
15	MRI-ESM2-0	native atmosphere TL159 gaussian grid (160x320 lat x lon) TL159; 320 x 160 longitude/latitude; 80 levels; top level 0.01 hPa	r1i1p1
16	NorESM2-LM	finite-volume grid with 1.9x2.5 degree lat/lon resolution 2 degree resolution; 144 x 96; 32 levels; top level 3 mb	r1i1p1
17	NorESM2-MM	finite-volume grid with 0.9x1.25 degree lat/lon resolution 1 degree resolution; 288 x 192; 32 levels; top level 3 mb	r1i1p1

Appendix B
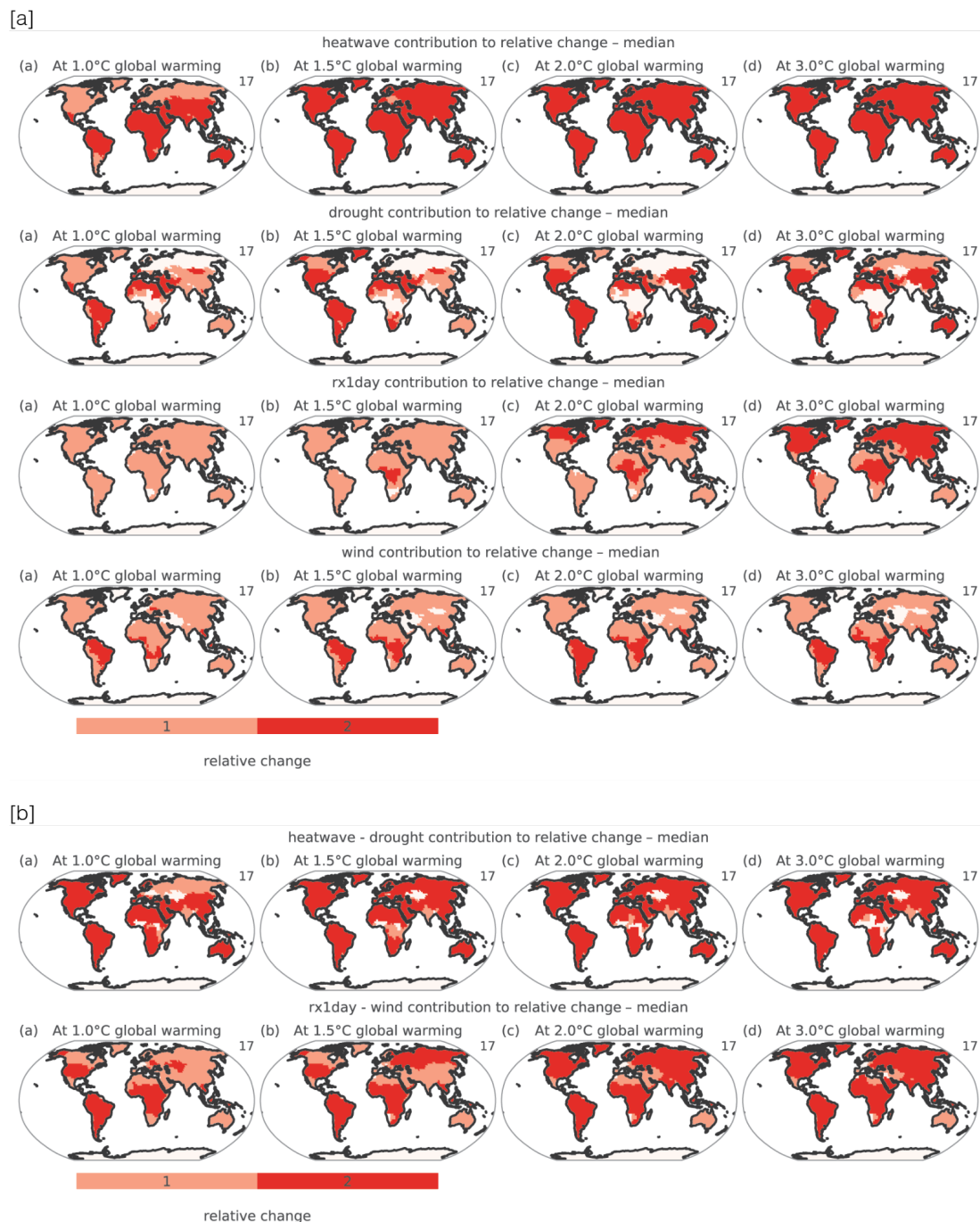
Figure B1. Show 20% relative change and 100% relative change as 1 and 2 for each individual extreme [a] and concurrent
440　extreme [b].
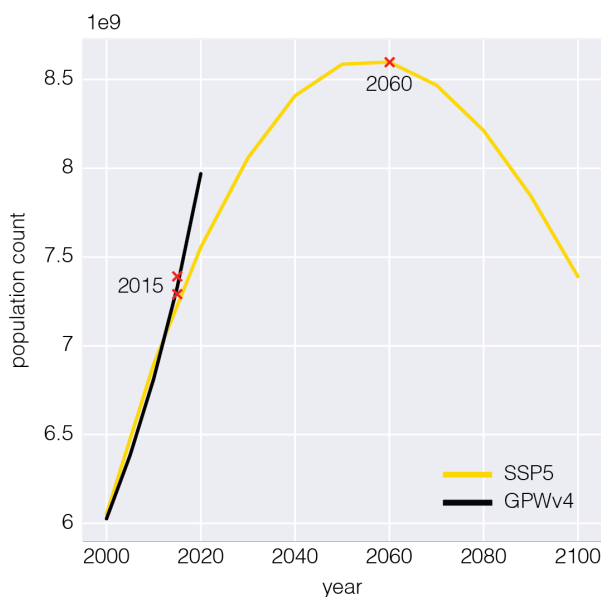
Figure B2. Global population counts for SSP5 and GPWv4 from 2000 to 2100. 2015 and 2060 population counts have been marked with x for both datasets.

445

7. Data availability

SSP5 and GPWv4 used for population analysis are provided by NASA Socioeconomic Data and Applications Center (sedac) and are available at https://sedac.ciesin.columbia.edu/data/set/popdynamics-1-8th-pop-base-year-projection-ssp-2000-2100-rev01 and https://sedac.ciesin.columbia.edu/data/set/gpw-v4-population -count-rev11 respectively.

450

8. Author contribution

FB, MH, and SIS planned the study; FB performed the analysis with support and guidance from MH and SIS; FB wrote the manuscript draft; MH and SIS reviewed and edited the manuscript. All authors were involved in discussions of the results and streamlining the text.

455

9. Competing interests

The contact author has declared that neither they nor their co-authors have any competing interests.

10. Acknowledgements

460

References

Alizadeh, M.R., Adamowski, J., Nikoo, M.R., AghaKouchak, A., Dennison, P., Sadegh, M., 2020. A century of observations
470   reveals   increasing   likelihood   of   continental-scale   compound   dry-hot   extremes.   Sci.   Adv.   6,   eaaz4571.
https://doi.org/10.1126/sciadv.aaz4571

Bathiany, S., Dakos, V., Scheffer, M., Lenton, T.M., 2018. Climate models predict increasing temperature variability in poor
countries. Sci. Adv. 4, eaar5809. https://doi.org/10.1126/sciadv.aar5809

Batibeniz, F., Ashfaq, M., Diffenbaugh, N.S., Key, K., Evans, K.J., Turuncoglu, U.U., Önol, B., 2020a. Doubling of U.S.
475   Population Exposure to Climate Extremes by 2050. Earths Future 8. https://doi.org/10.1029/2019EF001421

Batibeniz, F., Ashfaq, M., Önol, B., Turuncoglu, U.U., Mehmood, S., Evans, K.J., 2020b. Identification of major moisture
sources across the Mediterranean Basin. Clim. Dyn. 54, 4109–4127. https://doi.org/10.1007/s00382-020-05224-3

Bevacqua, E., Zappa, G., Lehner, F., Zscheischler, J., 2022. Precipitation trends determine future occurrences of compound
hot–dry events. Nat. Clim. Change. https://doi.org/10.1038/s41558-022-01309-5

480   Botzen, W.J.W., van den Bergh, J.C.J.M., Bouwer, L.M., 2010. Climate change and increased risk for the insurance sector: a
global perspective and an assessment for the Netherlands. Nat. Hazards 52, 577–598. https://doi.org/10.1007/s11069-009-
9404-1

Center for International Earth Science Information Network - CIESIN - Columbia University, 2018. Gridded Population of
the World, Version 4 (GPWv4): Population Count, Revision 11.

485   Champagne, O., Leduc, M., Coulibaly, P., Arain, M.A., 2020. Winter hydrometeorological extreme events modulated by
large-scale atmospheric circulation in southern Ontario. Earth Syst. Dyn. 11, 301–318. https://doi.org/10.5194/esd-11-301-
2020

Chiang, F., Mazdiyasni, O., AghaKouchak, A., 2018. Amplified warming of droughts in southern United States in
observations and model simulations. Sci. Adv. 4, eaat2380. https://doi.org/10.1126/sciadv.aat2380

490   Couasnon, A., Eilander, D., Muis, S., Veldkamp, T.I.E., Haigh, I.D., Wahl, T., Winsemius, H.C., Ward, P.J., 2020.
Measuring compound flood potential from river discharge and storm surge extremes at the global scale. Nat. Hazards Earth
Syst. Sci. 20, 489–504. https://doi.org/10.5194/nhess-20-489-2020

De Luca, P., Messori, G., Pons, F.M.E., Faranda, D., 2020. Dynamical systems theory sheds new light on compound climate
extremes in Europe and Eastern North America. Q. J. R. Meteorol. Soc. 146, 1636–1650. https://doi.org/10.1002/qj.3757

495   Dell, M., Jones, B.F., Olken, B.A., 2014. What Do We Learn from the Weather? The New Climate-Economy Literature. J. Econ. Lit. 52, 740–798. https://doi.org/10.1257/jel.52.3.740

Dell, M., Jones, B.F., Olken, B.A., 2012. Temperature Shocks and Economic Growth: Evidence from the Last Half Century. Am. Econ. J. Macroecon. 4, 66–95. https://doi.org/10.1257/mac.4.3.66

Diffenbaugh, N.S., Swain, D.L., Touma, D., 2015. Anthropogenic warming has increased drought risk in California. Proc.
500   Natl. Acad. Sci. 112, 3931–3936. https://doi.org/10.1073/pnas.1422385112

Eckstein, D., Künzel, V., Schafer, L., 2021. GLOBAL CLIMATE RISK INDEX 2021 Who Suffers Most from Extreme Weather Events? Westher-Related Loss Events in 2019 and 2000-2019. Germanwatch e.V.

Eyring, V., Bony, S., Meehl, G.A., Senior, C.A., Stevens, B., Stouffer, R.J., Taylor, K.E., 2016. Overview of the Coupled Model Intercomparison Project Phase 6 (CMIP6) experimental design and organization. Geosci. Model Dev. 9, 1937–1958.
505   https://doi.org/10.5194/gmd-9-1937-2016

Feng, S., Wu, X., Hao, Z., Hao, Y., Zhang, X., Hao, F., 2020. A database for characteristics and variations of global compound dry and hot events. Weather Clim. Extrem. 30, 100299. https://doi.org/10.1016/j.wace.2020.100299

Forzieri, G., Feyen, L., Russo, S., Vousdoukas, M., Alfieri, L., Outten, S., Migliavacca, M., Bianchi, A., Rojas, R., Cid, A., 2016. Multi-hazard assessment in Europe under climate change. Clim. Change 137, 105–119.
510   https://doi.org/10.1007/s10584-016-1661-x

Frame, D.J., Rosier, S.M., Noy, I., Harrington, L.J., Carey-Smith, T., Sparrow, S.N., Stone, D.A., Dean, S.M., 2020. Climate change attribution and the economic costs of extreme weather events: a study on damages from extreme rainfall and drought. Clim. Change 162, 781–797. https://doi.org/10.1007/s10584-020-02729-y

Guo, J., Kubli, D., Saner, P., Ronke, P., Institute, S.R., 2021. The Economics of Climate Change: No Action Not an Option.
515   Swiss Re Institute.

Hao, Z., Hao, F., Singh, V.P., Zhang, X., 2018. Changes in the severity of compound drought and hot extremes over global land areas. Environ. Res. Lett. 13, 124022. https://doi.org/10.1088/1748-9326/aaee96

Herrera-Estrada, J.E., Sheffield, J., 2017. Uncertainties in Future Projections of Summer Droughts and Heat Waves over the Contiguous United States. J. Clim. 30, 6225–6246. https://doi.org/10.1175/JCLI-D-16-0491.1
520   IPCC, 2021: Summary for Policymakers. In: Climate Change 2021: The Physical Science Basis. Contribution of Working Group I to the Sixth Assessment Report of the Intergovernmental Panel on Climate Change [Masson-Delmotte, V., P. Zhai, A. Pirani, S.L. Connors, C. Péan, S. Berger, N. Caud, Y. Chen, L. Goldfarb, M.I. Gomis, M. Huang, K. Leitzell, E. Lonnoy, J.B.R. Matthews, T.K. Maycock, T. Waterfield, O. Yelekçi, R. Yu, and B. Zhou (eds.)]. In Press.

Jahn, M., 2015. Economics of extreme weather events: Terminology and regional impact models. Weather Clim. Extrem. 10,
525   29–39. https://doi.org/10.1016/j.wace.2015.08.005

Jones, B., ONeill, B.C., 2020. Global One-Eighth Degree Population Base Year and Projection Grids Based on the Shared Socioeconomic Pathways, Revision 01.

23

Jones, B., O'Neill, B.C., 2016. Spatially explicit global population scenarios consistent with the Shared Socioeconomic Pathways. Environ. Res. Lett. 11, 084003. https://doi.org/10.1088/1748-9326/11/8/084003

530 Jones, B.F., Olken, B.A., 2010. Climate Shocks and Exports. Am. Econ. Rev. 100, 454–459. https://doi.org/10.1257/aer.100.2.454

Jones, P.W., 1999. First- and Second-Order Conservative Remapping Schemes for Grids in Spherical Coordinates. Mon. Weather Rev. 127, 2204–2210. https://doi.org/10.1175/1520-0493(1999)127<2204:FASOCR>2.0.CO;2

Kelebek, M.B., Batibeniz, F., Önol, B., 2021. Exposure Assessment of Climate Extremes over the Europe–Mediterranean

535 Region. Atmosphere 12, 633. https://doi.org/10.3390/atmos12050633

Kirono, D.G.C., Hennessy, K.J., Grose, M.R., 2017. Increasing risk of months with low rainfall and high temperature in southeast Australia for the past 150 years. Clim. Risk Manag. 16, 10–21. https://doi.org/10.1016/j.crm.2017.04.001

Kong, Q., Guerreiro, S.B., Blenkinsop, S., Li, X.-F., Fowler, H.J., 2020. Increases in summertime concurrent drought and heatwave in Eastern China. Weather Clim. Extrem. 28, 100242. https://doi.org/10.1016/j.wace.2019.100242

540 Li, L., Wang, R., Lv, G., Ning, L., Yuan, L., 2020. Likelihood of warm-season compound dry and hot extremes increased with stronger dependence (preprint). Climatology (Global Change). https://doi.org/10.1002/essoar.10505090.1

Li, L., Yao, N., Li, Y., Liu, D.L., Wang, B., Ayantobo, O.O., 2019. Future projections of extreme temperature events in different sub-regions of China. Atmospheric Res. 217, 150–164. https://doi.org/10.1016/j.atmosres.2018.10.019

Manning, C., Widmann, M., Bevacqua, E., Van Loon, A.F., Maraun, D., Vrac, M., 2019. Increased probability of compound

545 long-duration dry and hot events in Europe during summer (1950–2013). Environ. Res. Lett. 14, 094006. https://doi.org/10.1088/1748-9326/ab23bf

Martius, O., Pfahl, S., Chevalier, C., 2016. A global quantification of compound precipitation and wind extremes: COMPOUND PRECIPITATION AND WIND EXTREMES. Geophys. Res. Lett. 43, 7709–7717. https://doi.org/10.1002/2016GL070017

550 Mazdiyasni, O., AghaKouchak, A., 2015. Substantial increase in concurrent droughts and heatwaves in the United States. Proc. Natl. Acad. Sci. 112, 11484–11489. https://doi.org/10.1073/pnas.1422945112

Messmer, M., Simmonds, I., 2021. Global analysis of cyclone-induced compound precipitation and wind extreme events. Weather Clim. Extrem. 32, 100324. https://doi.org/10.1016/j.wace.2021.100324

Mukherjee, S., Mishra, A.K., 2021. Increase in Compound Drought and Heatwaves in a Warming World. Geophys. Res.

555 Lett. 48. https://doi.org/10.1029/2020GL090617

Mukherjee, S., Mishra, A.K., Mann, M.E., Raymond, C., 2021. Anthropogenic Warming and Population Growth May Double US Heat Stress by the Late 21st Century. Earths Future 9. https://doi.org/10.1029/2020EF001886

Poschlod, B., Zscheischler, J., Sillmann, J., Wood, R.R., Ludwig, R., 2020. Climate change effects on hydrometeorological compound events over southern Norway. Weather Clim. Extrem. 28, 100253. https://doi.org/10.1016/j.wace.2020.100253

560 Ranasinghe, R., A. C. Ruane, R. Vautard, N. Arnell, E. Coppola, F. A. Cruz, S. Dessai, A. S. Islam, M. Rahimi, D. Ruiz Carrascal, J. Sillmann, M. B. Sylla, C. Tebaldi, W. Wang, R. Zaaboul, 2021, Climate Change Information for Regional

Impact and for Risk Assessment. In: Climate Change 2021: The Physical Science Basis. Contribution of Working Group I to the Sixth Assessment Report of the Intergovernmental Panel on Climate Change [Masson-Delmotte, V., P. Zhai, A. Pirani, S. L. Connors, C. Péan, S. Berger, N. Caud, Y. Chen, L. Goldfarb, M. I. Gomis, M. Huang, K. Leitzell, E. Lonnoy, J. B. R.

565   Matthews, T. K. Maycock, T. Waterfield, O. Yelekçi, R. Yu and B. Zhou (eds.)]. Cambridge University Press. In Press.

Raveh-Rubin, S., Wernli, H., 2015. Large-scale wind and precipitation extremes in the Mediterranean: a climatological analysis for 1979-2012: Mediterranean Large-scale Wind and Precipitation Extremes. Q. J. R. Meteorol. Soc. 141, 2404–2417. https://doi.org/10.1002/qj.2531

Ridder, N.N., Pitman, A.J., Ukkola, A.M., 2021. Do CMIP6 Climate Models Simulate Global or Regional Compound Events

570   Skillfully? Geophys. Res. Lett. 48. https://doi.org/10.1029/2020GL091152

Ridder, N.N., Pitman, A.J., Westra, S., Ukkola, A., Do, H.X., Bador, M., Hirsch, A.L., Evans, J.P., Di Luca, A., Zscheischler, J., 2020. Global hotspots for the occurrence of compound events. Nat. Commun. 11, 5956. https://doi.org/10.1038/s41467-020-19639-3

Saeed, F., Schleussner, C., Ashfaq, M., 2021. Deadly Heat Stress to Become Commonplace Across South Asia Already at

575   1.5°C of Global Warming. Geophys. Res. Lett. 48. https://doi.org/10.1029/2020GL091191

Sarhadi, A., Ausín, M.C., Wiper, M.P., Touma, D., Diffenbaugh, N.S., 2018. Multidimensional risk in a nonstationary climate: Joint probability of increasingly severe warm and dry conditions. Sci. Adv. 4, eaau3487. https://doi.org/10.1126/sciadv.aau3487

Schubert, S.D., Wang, H., Koster, R.D., Suarez, M.J., Groisman, P.Ya., 2014. Northern Eurasian Heat Waves and Droughts.

580   J. Clim. 27, 3169–3207. https://doi.org/10.1175/JCLI-D-13-00360.1

Schwingshackl, C., Sillmann, J., Vicedo-Cabrera, A.M., Sandstad, M., Aunan, K., 2021. Heat Stress Indicators in CMIP6: Estimating Future Trends and Exceedances of Impact-Relevant Thresholds. Earths Future 9. https://doi.org/10.1029/2020EF001885

Sedlmeier, K., Feldmann, H., Schädler, G., 2018. Compound summer temperature and precipitation extremes over central

585   Europe. Theor. Appl. Climatol. 131, 1493–1501. https://doi.org/10.1007/s00704-017-2061-5

Seneviratne, S.I., Corti, T., Davin, E.L., Hirschi, M., Jaeger, E.B., Lehner, I., Orlowsky, B., Teuling, A.J., 2010. Investigating soil moisture–climate interactions in a changing climate: A review. Earth-Sci. Rev. 99, 125–161. https://doi.org/10.1016/j.earscirev.2010.02.004

Seneviratne, S.I., Donat, M.G., Pitman, A.J., Knutti, R., Wilby, R.L., 2016. Allowable CO2 emissions based on regional and

590   impact-related climate targets. Nature 529, 477–483. https://doi.org/10.1038/nature16542

Seneviratne, S.I., Hauser, M., 2020. Regional Climate Sensitivity of Climate Extremes in CMIP6 Versus CMIP5 Multimodel Ensembles. Earths Future 8. https://doi.org/10.1029/2019EF001474

Sharma, S., Mujumdar, P., 2017. Increasing frequency and spatial extent of concurrent meteorological droughts and heatwaves in India. Sci. Rep. 7, 15582. https://doi.org/10.1038/s41598-017-15896-3

595   Singh, J., Ashfaq, M., Skinner, C.B., Anderson, W.B., Singh, D., 2021. Amplified risk of spatially compounding droughts during co-occurrences of modes of natural ocean variability. Npj Clim. Atmospheric Sci. 4, 7. https://doi.org/10.1038/s41612-021-00161-2

Tilloy, A., Malamud, B., Joly-Laugel, A., 2021. A Methodology for the Spatiotemporal Identification of Compound Hazards: Wind and Precipitation Extremes in Great Britain (1979–2019) (preprint). Dynamics of the Earth system: models.
600   https://doi.org/10.5194/esd-2021-52

UNFCCC, U., 2015. Paris Agreement.

United Nations, Department of Economic and Social Affairs, Population Division, 2019. World urbanization prospects: the 2018 revision.

Vogel, M.M., Hauser, M., Seneviratne, S.I., 2020. Projected changes in hot, dry and wet extreme events' clusters in CMIP6
605   multi-model ensemble. Environ. Res. Lett. 15, 094021. https://doi.org/10.1088/1748-9326/ab90a7

Vogel, M.M., Orth, R., Cheruy, F., Hagemann, S., Lorenz, R., Hurk, B.J.J.M., Seneviratne, S.I., 2017. Regional amplification of projected changes in extreme temperatures strongly controlled by soil moisture-temperature feedbacks. Geophys. Res. Lett. 44, 1511–1519. https://doi.org/10.1002/2016GL071235

Wartenburger, R., Hirschi, M., Donat, M.G., Greve, P., Pitman, A.J., Seneviratne, S.I., 2017. Changes in regional climate
610   extremes as a function of global mean temperature: an interactive plotting framework. Geosci. Model Dev. 10, 3609–3634. https://doi.org/10.5194/gmd-10-3609-2017

Wu, S., Chan, T.O., Zhang, W., Ning, G., Wang, P., Tong, X., Xu, F., Tian, H., Han, Y., Zhao, Y., Luo, M., 2021. Increasing Compound Heat and Precipitation Extremes Elevated by Urbanization in South China. Front. Earth Sci. 9, 636777. https://doi.org/10.3389/feart.2021.636777

615   Yu, R., Zhai, P., 2020. More frequent and widespread persistent compound drought and heat event observed in China. Sci. Rep. 10, 14576. https://doi.org/10.1038/s41598-020-71312-3

Zhou, P., Liu, Z., 2018. Likelihood of concurrent climate extremes and variations over China. Environ. Res. Lett. 13, 094023. https://doi.org/10.1088/1748-9326/aade9e

Zscheischler, J., Martius, O., Westra, S., Bevacqua, E., Raymond, C., Horton, R.M., van den Hurk, B., AghaKouchak, A.,
620   Jézéquel, A., Mahecha, M.D., Maraun, D., Ramos, A.M., Ridder, N.N., Thiery, W., Vignotto, E., 2020. A typology of compound weather and climate events. Nat. Rev. Earth Environ. 1, 333–347. https://doi.org/10.1038/s43017-020-0060-z

Zscheischler, J., Naveau, P., Martius, O., Engelke, S., Raible, C.C., 2021. Evaluating the dependence structure of compound precipitation and wind speed extremes. Earth Syst. Dyn. 12, 1–16. https://doi.org/10.5194/esd-12-1-2021

Zscheischler, J., Seneviratne, S.I., 2017. Dependence of drivers affects risks associated with compound events. Sci. Adv. 3,
625   e1700263. https://doi.org/10.1126/sciadv.1700263